Nature of Cysteine-Based Re(V)═O(N_2S_2) Radiopharmaceuticals at Physiological pH Ascertained by Investigation of a New Complex with a *Meso* N_2S_2 Ligand Having Carboxyl Groups Anti to the Oxo Group

Lory Hansen,[†] Shun Hirota,[‡] Xiaolong Xu,[†] Andrew T. Taylor,[†] and Luigi G. Marzilli*,[⊥]

Departments of Radiology and Chemistry, Emory University, Atlanta, Georgia 30322, and Department of Chemistry, Graduate School of Science, Nagoya University, Chikusa-ku, Nagoya 464-01, Japan

Received February 18, 2000

X-ray structural characterization of a new isomer of ReO(TMECH_3) revealed that it is *anti*-ReO(DL-TMECH_3) (**1**). (DL-TMECH_6 is *meso*-tetramethyl-ethylene-dicysteine prepared from racemic penicillamine (penH_4), the subscript on H indicating the number of dissociable protons; anti denotes the geometric isomer having both carboxyl groups anti to the oxo ligand.) In **1**, one carboxyl is deprotonated and coordinated trans to the oxo ligand, and the other is protonated and dangling. The ^{1}H NMR spectrum (assigned by 2D methods) of **1** at pH 4 in aqueous solution revealed that the structure of **1** is the same as in the solid state except for deprotonation of the dangling carboxyl group, affording the monoanion. All chelate ring protons and methyl groups are inequivalent and give sharp signals. As the pH was raised above 7, the 1D ^{1}H NMR signals of the monoanion broadened. Broadening was severe for the methyl and ethylene signals of the tridentate half of the monoanion, and these signals were replaced by new signals for the dianion. The changes suggested a rate process that was intermediate on the NMR time scale, such as CO_2^- ligation/deligation. With increasing pH the dianion signals sharpened up to pH ∼8 and then broadened up to pH ≈ 10. Finally, the spectrum at pH 10.8 showed only half the number of signals. Each signal was at the midpoint shift between two corresponding signals observed at lower pH, indicating a time averaging between the halves of the DL-TMEC ligand, but no change in protonation state. Two Re═O stretching bands (923 and 933 cm^{-1}) with a constant intensity ratio of ∼1 were observed for the dianion. These results can be explained if the dianion exists detectably only as a NH-deprotonated/carboxyl-deligated form having two conformers. The conformers differ in the N lone pair (NLp) orientation (either endo or exo with respect to the oxo ligand) and thus have slightly different Re═O stretching frequencies. Although they can be detected by resonance Raman spectroscopy, the conformers are indistinguishable by NMR spectroscopy because NLp inversion (and hence conformer interconversion) is very fast. Interchange of the NH and NLp sites affects the NMR spectra. At pH 8.3 the signals of the dianion are sharpest because interchange is slowest. Below and above pH 8.3, the signals are broader because acid and base catalysis, respectively, increase the rate of interchange between the NH and NLp sites.

Introduction

In aqueous solution, hydroxide can act as a ligand or can deprotonate a coordinated ligand. Having encountered this ambiguity in our studies of radiopharmaceuticals, we are exploring the use of NMR and resonance Raman spectroscopy applied to complexes with selected symmetries to develop criteria for predicting the effect of hydroxide on structure at physiological pH. Although this is an interesting intellectual challenge, there are practical consequences as well. Specifically, we need to know the form that the radiopharmaceutical adopts so that we can design appropriate new generations of useful diagnostic agents.

We are investigating the factors dictating both the structures and the solution chemistry of Re(V)═O(N_2S_2) complexes with ligands derived from cysteine (cys).[1−8] The impetus for our studies is that the ^{99m}Tc tracer agent formed from LL-ECH$_6$ exhibits behavior in vivo that is useful for renal imaging in nuclear medicine.[9,10] (LL-ECH$_6$ is ethylene-di-L-cysteine (Chart 1); the subscript on H indicates the number of dissociable OH + NH + SH protons.) More recent work with the tracer formed

[†] Department of Radiology, Emory University.
[‡] Nagoya University.
[⊥] Department of Chemistry, Emory University.

(1) Marzilli, L. G.; Hansen, L.; Kuklenyik, Z.; Cini, R.; Banaszczyk, M. G.; Taylor, A., Jr. In *Technetium and Rhenium in Chemistry and Nuclear Medicine 4*; Nicolini, M., Bandoli, G., Mazzi, U., Eds.; SGEditoriali: Padova, 1995; pp 27−32.
(2) Marzilli, L. G.; Banaszczyk, M. G.; Hansen, L.; Kuklenyik, Z.; Cini, R.; Taylor, A., Jr. *Inorg. Chem.* **1994**, *33*, 4850−4860.
(3) Hansen, L.; Yue, K. T.; Xu, X.; Lipowska, M.; Taylor, A., Jr.; Marzilli, L. G. *J. Am. Chem. Soc.* **1997**, *38*, 8965−8972.
(4) Hansen, L.; Lipowska, M.; Taylor, A., Jr.; Marzilli, L. G. *Inorg. Chem.* **1995**, *34*, 3579−3580.
(5) Hansen, L.; Xu, X.; Yue, K. T.; Kuklenyik, Z.; Taylor, A., Jr.; Marzilli, L. G. *Inorg. Chem.* **1996**, *35*, 1958−1966.
(6) Hansen, L.; Xu, X.; Yue, K. T.; Taylor, A., Jr.; Marzilli, L. G. *Inorg. Chem.* **1996**, *35*, 2785−2791.
(7) Hansen, L.; Lipowska, M.; Melendez, E.; Xu, X.; Hirota, S.; Taylor, A. T.; Marzilli, L. G. *Inorg. Chem.* **1999**, *38*, 5351−5358.
(8) Hansen, L.; Xu, X.; Lipowska, M.; Taylor, A., Jr.; Marzilli, L. G. *Inorg. Chem.* **1999**, *38*, 2890−2897.
(9) Taylor, A., Jr.; Hansen, L.; Eshima, D.; Malveaux, E. J.; Folks, R.; Shattuck, L.; Lipowska, M.; Marzilli, L. G. *J. Nucl. Med.* **1997**, *38*, 821−826.
(10) Van Nerom, C. G.; Bormans, G. M.; De Roo, M.; Verbruggen, A. M. *Eur. J. Nucl. Med.* **1993**, *20*, 738−746.

10.1021/ic000183q CCC: $19.00
Published on Web 11/11/2000

Chart 1

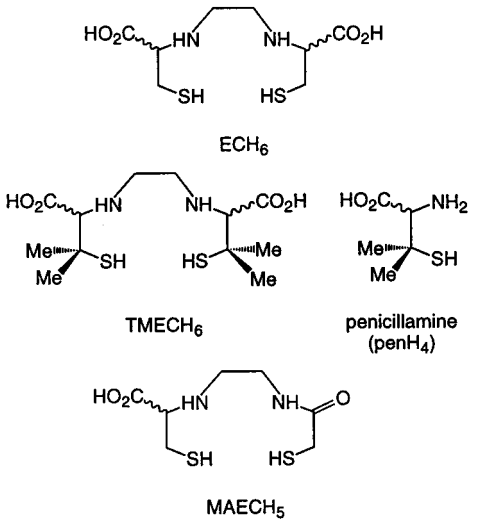

from DD-ECH_6 shows even more promise.[9,11] Identification of the chemical properties that promote such behavior should facilitate the development of new radiopharmaceuticals. Near physiological pH, the tracer exists as a mixture of ^{99m}TcO(LL-ECH_2)$^-$ (with both carboxyl and both thiol groups deprotonated) and ^{99m}TcO(LL-ECH)$^{2-}$ (with one NH group deprotonated); the apparent pK_a of the monoanion is 6.6, leading to mono- (~20%) and dianionic (~80%) forms. Initially, typical five-coordinate Tc(V)=O complexes had been proposed for both charged forms.[12] However, supporting experimental data were lacking, and the extremely broad ^{1}H NMR spectra observed for ^{99}TcO(LL-ECH_3) and ReO(LL-ECH_3) near physiological pH suggested that the situation was not so simple.[2,12] We studied ReO(LL-ECH_3) by using X-ray crystallography and spectroscopic methods,[2] and we prepared ReO(DD-$TMECH_3$)[1,2] and ReO(D-$penH_2$)(D-$penH_3$)[5] to obtain species with simplified ^{1}H spin systems providing more informative NMR spectra. ($TMECH_6$ is tetramethyl-ECH_6, prepared from penicillamine ($penH_4$) (Chart 1)).

Our investigations showed that at physiological pH the minor (monoanionic) form of these EC-type complexes is a six-coordinate carboxyl-ligated species with neither NH group deprotonated (Scheme 1). (The EC ligand is shown in the schemes and charts for clarity.) Although the weight of evidence suggested very strongly that the major (dianionic) form was carboxyl-deligated, the symmetry of the complex made tentative our conclusion that the major form was a five-coordinate species with the *anti*-N-deprotonated (bottom left, Scheme 1). Specifically, the alternative formulation with OH^- axially ligated and neither NH group deprotonated (bottom right, Scheme 1) could not be excluded. With the DD and LL EC-type ligands, one carboxyl group is syn while the other is anti to the oxo ligand (Chart 2). For any reasonable formulation, the dianions always have two sets of cys/pen NMR signals.

The uncertainties surrounding the structure of the dianion prompted us to investigate *meso*-EC- and pen-type ligands.[3,4,6] Complexes of such ligands are important for eventually ascertaining the influence of ligand stereochemistry on renal

Scheme 1. Equilibria of Complexes with Chiral-EC-Type Ligands (LL-EC Is Shown)

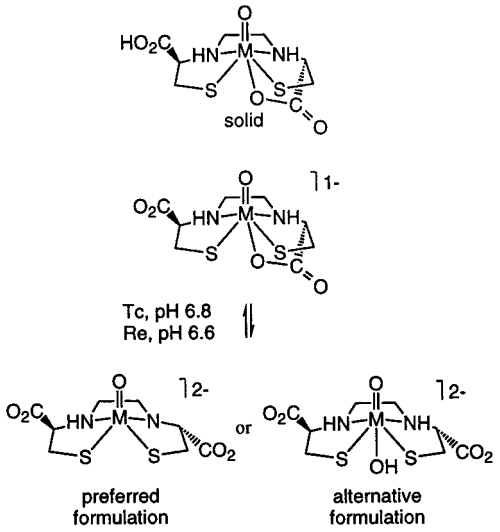

Chart 2

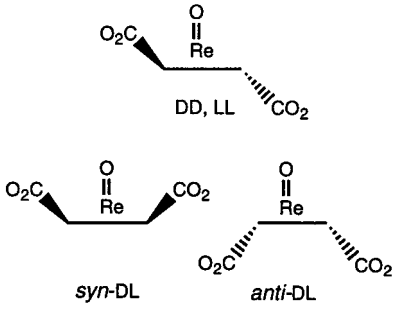

clearance. In complexes with meso ligands (DL), the two carboxyl groups are oriented to the same side of the basal plane (Chart 2). Two families of complexes are possible with the oxo ligand and carboxyl groups either syn or anti. At high pH and under reflux, only the syn isomers of the EC-type complexes were isolated. The same behavior was found for a related MAMA-type complex (MAMA = monoamine-monoamide-dithiol), ReO($MAECH_2$) ($MAECH_5$ is mercaptacetamide-ethylene-cysteine, Chart 1).[7] We subsequently discovered that the anti isomers of the EC- and MAEC-type complexes formed under milder pH conditions. However, they were relatively unstable, converting to the syn isomers, and difficult to isolate and characterize. We prepared *syn*-ReO(DL-$TMECH_3$) for NMR investigations by ligand exchange of $ReIO_2(PPh_3)_2$ with DL-$TMECH_6$. Formation of *anti*-ReO(DL-$TMECH_3$) was detected under mild pH conditions. However, in this single case the anti isomer converted to the syn isomer only at pH values >10 and at a slow rate ($t_{1/2}$ of hours), and the anti isomer could be isolated on a preparative scale by column chromatography. The unusually slow isomerization of *anti*-ReO(DL-$TMECH_3$) provided an almost unique opportunity to isolate an anti isomer and to study in detail the structural and solution chemistry of this elusive isomeric form.

Experimental Section

Ethylene-di-penicillamine (tetramethyl-ECH_6, $TMECH_6$) was prepared according to known methods[13,14] from racemic penicillamine; the resulting mixture of DD, LL, and DL isomers was isolated. $ReIO_2$-

(11) Hansen, L.; Marzilli, L. G.; Taylor, A. *Q. J. Nucl. Med.* **1998**, *42*, 280−293.
(12) Edwards, D. S.; Cheesman, E. H.; Watson, M. W.; Maheu, L. J.; Nguyen, S. A.; Dimitre, L.; Nason, T.; Watson, A. D.; Walovitch, R. In *Technetium and Rhenium in Chemistry and Nuclear Medicine 3*; Nicolini, M., Bandoli, G., Mazzi, U., Eds.; Cortina International: Verona, Italy, 1990; pp 433−444.
(13) Blondeau, P.; Berse, C.; Gravel, D. *Can. J. Chem.* **1967**, *45*, 49−52.
(14) Ratner, S.; Clarke, H. T. *J. Am. Chem. Soc.* **1937**, *59*, 200−206.

Table 1. Crystallographic Data for *anti*-ReO(DL-$TMECH_3$)·H_2O (**1**)

emp form	$C_{12}H_{21}N_2O_6ReS_2$
fw	539.6
T (K)	293
λ (Å)	0.71073
space group	$P2_12_12_1$
unit cell dimens	
a (Å)	9.7500 (10)
b (Å)	11.413 (2)
c (Å)	15.657 (3)
V (Å^3)	1742.3 (5)
Z	4
ρ_{calcd} mg m^{-3}	2.07
abs coeff (mm^{-1})	7.24
R indices [$I > 2\sigma(I)$][a]	R1 = 0.0365, wR2 = 0.0951
R indices (all data)[a]	R1 = 0.0369, wR2 = 0.0956

[a] R1 = $(\sum||F_o| - |F_c||)/\sum|F_o|$. wR2 = $[\sum[w(F_o^2 - F_c^2)^2]/\sum[w(F_o^2)^2]]^{1/2}$, where $w = 1/[\sigma^2(F_o^2) + (aP)^2 + bP]$ and $P = [(\max;0,F_o^2) + 2F_c^2]/3$.

$(PPh_3)_2$[15] was prepared as previously reported. Elemental analysis was performed by Atlantic Microlabs, Atlanta, GA. Cation exchange column chromatography was performed with Bio-Rad AG 50WX4 200−400 mesh analytical grade resin equilibrated with 1 N HCl.

Syntheses. *anti*-ReO(DL-$TMECH_3$)·H_2O (1). $TMECH_6$ (0.20 g, 0.6 mmol) was dissolved in 50% MeOH/H_2O (40 mL) by adjusting the pH to 7 with 1 N NaOH. $ReIO_2(PPh_3)_2$ (0.43 g, 0.5 mmol) was added, and the reaction mixture was heated at reflux for 1 h. The resulting rose solution was cooled to 25 °C and analyzed by HPLC [Beckman Ultrasphere ODS 5 μm, 4.6 × 250 mm column; 6% EtOH, 0.01 M NaH_2PO_4, pH 7.0 mobile phase; flow rate of 1 mL/min; UV detector (254 nm)]. The isomer distribution was ∼60% DD+LL, ∼10% *syn*-DL, and ∼30% *anti*-DL (**1**). (Chromatogram peaks corresponding to the DD+LL and *syn*-DL products were identified by spiking the samples with purified DD+LL[2] or *syn*-DL[3] species.) The solution was acidified to pH 2 with concentrated HCl, reduced in volume to ∼10 mL by rotary evaporation, and filtered. Species **1** was separated from the DD+LL and *syn*-DL isomers by cation exchange column chromatography by eluting with 1 N HCl. The DD+LL isomers eluted first, followed by **1**; the *syn*-DL isomer remained on the column. The fraction containing **1** was collected and adsorbed by using a Whatman SPE ODS-4 cartridge, primed with MeOH. The cartridge was washed with H_2O and eluted with MeOH. The pink eluent was evaporated to near dryness. The violet microcrystals that formed were collected, washed with H_2O, and vacuum dried: yield, 12 mg (4%). Anal. Calcd for $C_{12}H_{21}N_2O_6ReS_2$: C, 26.71; H, 3.92; N, 5.19. Found: C, 26.70; H, 4.16; N, 5.14.

X-ray Crystallography. Crystals of *anti*-ReO(DL-$TMECH_3$)·H_2O (**1**) suitable for X-ray diffraction were grown by slow diffusion of HCl vapors into a solution of **1** (prepared by dissolving the solid in H_2O with dropwise addition of 1 N NaOH). A violet crystal cut from a star cluster with dimensions of 0.30 × 0.48 × 0.40 mm^3 was used for data collection. Intensity data were collected at room temperature on a Siemens P4 instrument. The crystal system and high-angle cell constants were determined by automatic reflection selection, indexing, and least-squares refinement. Three check reflections were measured every 97 reflections; there was no significant deviation in intensities. Intensity data were corrected for Lorentz and monochromator polarization and absorption (semiempirical method based on azimuthal scans). The structure of **1** was solved by Patterson methods and refined by full-matrix least-squares procedures on F^2 using SHELXL 93. All non-hydrogen atoms were refined anisotropically. The amine, carboxylic, and water H-atoms were located from difference maps and refined with idealized bond lengths (d(N−H) = 0.90 Å, d(O−H) = 0.85 Å). All other H-atoms were generated at calculated positions (d(C−H) = 0.96 Å) and refined using a riding model with isotropic thermal parameters that were 20% greater than the U(eq) of the bonded heavy atom. Crystal data and refinement parameters for **1** are presented in Table 1.

(15) Ciani, G. F.; D'Alfonso, G.; Romiti, P. F.; Sironi, A.; Freni, M. *Inorg. Chim. Acta* **1983**, *72*, 29−37.

NMR Spectroscopy. NMR spectra were recorded in D_2O at room temperature; chemical shifts (ppm) were referenced to (trimethylsilyl)-propionic acid (TSP). Variable pH (uncorrected) spectra were recorded with Nicolet NT 360 or GE GN-600 Omega (128 scans) spectrometers. The pH was adjusted with NaOD and DCl.

Signal assignments for **1** at pH 4.3 were determined from a ^{1}H−^{13}C heteronuclear multiple bond correlation (HMBC) spectrum acquired on a GE GN-600 Omega NMR at room temperature; chemical shifts were referenced to the 1D ^{1}H and ^{13}C NMR spectra; 2048 t_2 and 256 t_1 points were collected with 160 scans. Data were processed with FELIX (Hare Research, Inc.), zero-filled to 2048 points in the t_1 dimension, shifted by a sine bell window function (40° t_2, 10° t_1), and Fourier transformed. Procedures are described in more detail in refs 2 and 3.

Resonance Raman Spectroscopy. pH Dependence. Raman scattering was excited at 406.7 nm by a Kr^+ ion laser (Spectra Physics, Model 2016) and detected with a cooled CCD (Astromed CCD, 3200) attached to a single polychromator (Ritsu Oyo Kogaku, DG-1000). A slit width of 200 μm (spectral slit width of 8 cm^{-1}) and a slit height of 10 mm were used. The laser power and width at the sample point were 12 mW and ∼50 mm, respectively. All measurements were carried out at room temperature with a spinning cell (3500 rpm) to avoid photodecomposition. Accumulation time for each sample was 500 s. Raman shifts were calibrated with CH_3CN and acetone as standards. Uncertainty of the Raman bands was ± 1 cm^{-1}. Species **1** was dissolved to a concentration of 15 mM with D_2O. The solution was first raised to alkaline pH to dissolve the complex completely and then adjusted to pH 6.4. The Raman measurement was made and then the pH (uncorrected) of the solution was raised stepwise to higher pH values for subsequent measurements. The pH was adjusted by adding NaOD (110 mg dissolved in 1 mL of D_2O) and concentrated DCl (Sigma).

^{18}O Exchange. Measurements were made with excitations at 406.7 nm from a Kr^+ laser (Coherent Innova 100). Power at the samples was kept below 20 mW. Signals were collected via 90° geometry by a triple monochromator (Spex 1877 Triplemate) with a photodiode array detector (IRY-1024 detector and ST-120 controller, Princeton Instruments). Raman shifts were calibrated with a toluene standard. Peak positions were accurate to within ±1−2 cm^{-1}. Typical resolution was 6−8 cm^{-1}. *anti*-ReO(DL-$TMECH_3$) and *syn*-ReO(DL-$TMECH_3$)[3] were dissolved in D_2O (0.5 mL) to a concentration of ∼5 mM. The pH of each solution was adjusted to pH 12.5 by addition of NaOD (40% w/v), and the samples were immediately freeze-dried. Each residue (0.5−1.0 mg) was dissolved in $H_2{}^{18}O$ (97.3%, 25 μL) and $H_2{}^{16}O$ (25 μL) (control) and allowed to stand (3 d for *anti*-ReO(DL-$TMECH_3$), ∼6 h for *syn*-ReO(DL-$TMECH_3$)).

Results

Descriptive indicators used in this work are as follows: subscripted b and t indicate bidentate and tridentate, respectively; endo (′) and exo (″) indicate atoms or groups near and away from the oxo ligand, respectively.

Syntheses. Ligand exchange of the isomeric mixture of $TMECH_6$ with $ReIO_2(PPh_3)_2$ resulted in the formation of a mixture of ReO($TMECH_3$) isomers. The percentage of total product formed was always ∼60% DD+LL and ∼40% *syn*-DL+*anti*-DL by HPLC. However, the *syn*-DL:*anti*-DL ratio varied with pH. At pH values >10 the *syn*-DL:*anti*-DL ratio was >1, and the ratio increased with prolonged reaction times. At lower pH values (pH 7−8) ∼30% of the product formed was *anti*-ReO(DL-$TMECH_3$) (**1**). Species **1** was obtained after separation by column chromatography from the DD+LL and the *syn*-DL isomers.

X-ray Crystallography. A perspective drawing of **1** appears in Figure 1. Selected bond lengths and bond angles are listed in Table 2. The structure of **1** has a typical N_2S_2 basal donor set with a deprotonated carboxyl group bound trans to the oxo ligand. The second carboxyl group is protonated and dangling.

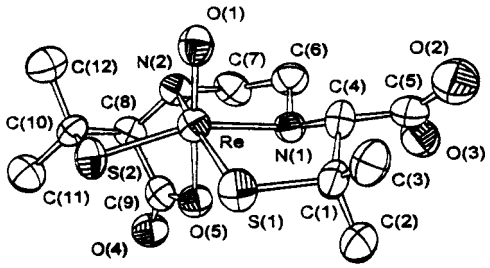

Figure 1. Perspective drawing of *anti*-ReO(DL-TMECH$_3$) (**1**) with 50% probability for the thermal ellipsoids.

Table 2. Selected Bond Distances (Å) and Bond Angles (deg) for *anti*-ReO(DL-TMECH$_3$)·H$_2$O (**1**)

Bond Distances			
Re−O(1)	1.701(9)	Re−N(2)	2.179(9)
Re−O(5)	2.200(8)	Re−S(1)	2.249(3)
Re−N(1)	2.139(8)	Re−S(2)	2.285(3)
Bond Angles			
O(1)−Re−N(1)	96.7(4)	N(1)−Re−S(2)	155.3(3)
O(1)−Re−N(2)	88.5(4)	N(2)−Re−S(2)	88.8(2)
N(1)−Re−N(2)	82.5(4)	O(5)−Re−S(2)	80.3(2)
O(1)−Re−O(5)	157.8(3)	S(1)−Re−S(2)	98.83(12)
N(1)−Re−O(5)	75.0(3)	C(1)−S(1)−Re	103.0(4)
N(2)−Re−O(5)	70.1(3)	C(10)−S(2)−Re	97.6(4)
O(1)−Re−S(1)	105.9(3)	C(6)−N(1)−Re	105.9(6)
N(1)−Re−S(1)	83.4(3)	C(4)−N(1)−Re	107.7(6)
N(2)−Re−S(1)	160.9(3)	C(7)−N(2)−Re	107.8(7)
O(5)−Re−S(1)	93.8(2)	C(8)−N(2)−Re	103.5(6)
O(1)−Re−S(2)	106.1(3)	C(9)−O(5)−Re	116.3(7)

The Re−N and Re−S bond lengths in **1** fall within normal ranges (Table 2).[2,3,16] The Re═O and Re−O distances are within statistical significance of structurally related six-coordinate M(V)═O(N$_2$S$_2$) complexes, ReO(LL-ECH$_3$),[2] [^{99}TcO(*N,N*′-ethylene-bis(acetylacetone-thioimine)H$_2$O]Cl,[17] and ^{99}TcO(D-penH$_2$)(D-penH$_3$).[16] However, the Re═O bond (1.701 (9) Å) is numerically longer, and the Re−O bond (2.200 (8) Å) is numerically shorter in **1** compared to the corresponding bond distances in these other complexes: Re═O, 1.643(3)−1.688(10) Å; Re−O 2.214(4)−2.384(3) Å.

The Re atom is displaced by 0.38 Å toward the oxo ligand and out of the basal plane defined by N(1), N(2), S(1), and S(2). Such an approximately 0.4 Å displacement is typically found in related six-coordinate Re(V)═O complexes.[2,17] Normally, this displacement causes all four *cis*-O═Re−N/S bond angles to be ∼94° or greater. However, in **1** the *cis*-O═Re−N(2) bond angle is acute (88.5(4)°). In ReO(LL-ECH$_3$),[2] a complex closely related to **1**, the *cis*-O═Re−N/S bond angles range from 93.9(5)° to 109.4(4)°. Like **1**, ReO(LL-ECH$_3$) has a N$_2$S$_2$ basal ligand arrangement, one CO_2^- bound trans to the oxo group, and an *endo*-NH belonging to cys$_t$. This *endo*-NH orientation gives the cys$_t$ chelate ring a conformation that positions the CO_2^- within bonding distance of Re. However, the NH belonging to the pen$_b$/cys$_b$ residue is exo in **1** and endo in ReO(LL-ECH$_3$). The pen$_b$ C$_\alpha$ chirality is opposite to that of the cys$_b$ C$_\alpha$ chirality. Hence, the opposite N$_b$ configuration extends the dangling CO_2H away from the inner coordination sphere and the ligated CO_2^- group. Because the stereochemistry of the two N's is *exo*-NH/*endo*-NH in **1** and *endo*-NH/*endo*-NH in ReO(LL-ECH$_3$), the N−C$_{en}$−C$_{en}$−N (C$_{en}$ = ethylene C atom) torsion angle is much larger in **1** (68°) than in ReO(LL-ECH$_3$) (44°). The large pucker in the ethylene chelate ring of **1** positions N(2) 0.3 Å above the best-fit plane of the other three basal donors; this position of N(2) results in a small *cis*-O═Re−N(2) bond angle.

Chart 3

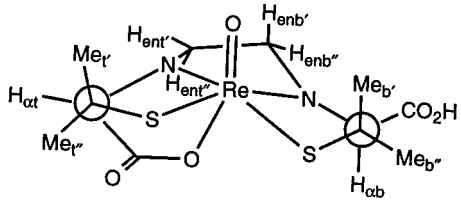

Chart 4

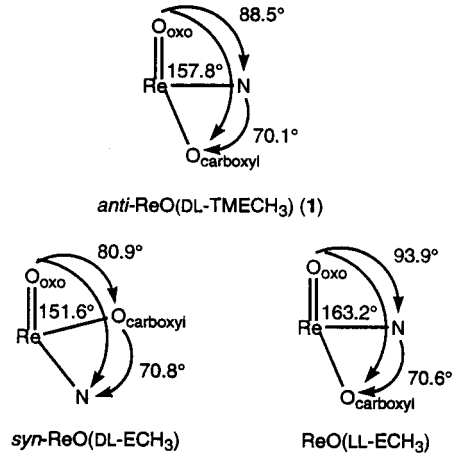

The pen$_t$/cys$_t$ residues in **1**, *syn*-ReO(DL-ECH$_3$),[4] and ReO(LL-ECH$_3$)[2] have different stereochemical features and hence significantly different *cis*-O═Re−N/O$_{carboxyl}$ and *trans*-O═Re−N/O$_{carboxyl}$ bond angles (Chart 4). However, within the pen$_t$/cys$_t$ residue, the *cis*-N−Re−O$_{carboxyl}$ bond angles (70.1° in **1**; 70.6° in ReO(LL-ECH$_3$); 70.8° in *syn*-ReO(DL-ECH$_3$)) are very similar. This highly preserved structural feature suggests that the quinquedentate ligands have rigid coordination constraints. The corresponding bond angle in ^{99}TcO(D-penH$_3$)(D-penH$_2$) was 91.1°.[16]

NMR Spectroscopy. Signal Assignments. The HMBC spectrum of **1** was acquired at pH 4.3 for two reasons. First, at this pH the complex has good solubility in D$_2$O. Second, the ^{1}H signals of the complex are sharpest (more noticeable at low field strengths, 360 MHz) and well separated except for the two downfield Me singlets. The presence of two sets of ^{1}H and ^{13}C signals, one for each half of the TMEC ligand, is consistent with the coordination geometry found for the neutral form in the solid state, i.e., with one carboxyl group ligated and the second dangling. (Atom labeling is shown in Chart 3.) Signals from the same half of the ligand were identified by H$_\alpha$−CO$_2$, H$_\alpha$−C$_{Me}$, H$_\alpha$−C$_\beta$, H$_{Me}$−C$_\alpha$, H$_{Me}$−C$_\beta$, H$_{Me}$−C$_{Me}$ and H$_\alpha$−C$_{en}$ (en = ethylene) cross-peaks. To determine which signals belonged to the bidentate N,S-pen residue (pen$_b$) and tridentate-N,S,O-pen residue (pen$_t$), cross-peak intensities were correlated with the torsion angles observed in the solid state. One strong H$_\alpha$-C$_{Me}$ HMBC cross-peak was observed, consistent with a *trans*-H$_\alpha$−C$_\alpha$−C$_\beta$−C$_{Me}$ torsion angle. In the solid state, the H$_\alpha$−C$_\alpha$−C$_\beta$−C$_{Me''}$ torsion angle of pen$_b$ was trans (Figure 1), whereas both H$_\alpha$−C$_\alpha$−C$_\beta$−C$_{Me}$ torsion angles of pen$_t$ were gauche. Thus, the set of signals having the strongly correlated H$_\alpha$ and C$_{Me''}$ cross-peak was assigned to pen$_b$. The other set of signals was assigned to pen$_t$. For the ethylene bridge, C$_6$ and C$_7$ were assigned from the respective cross-peaks to H$_\alpha$. Cross-

(16) Franklin, K. J.; Howard-Lock, H. E.; Lock, C. J. L. *Inorg. Chem.* **1982**, *21*, 1941−1946.
(17) Stassinopoulou, C. I.; Mastrostamatis, S.; Papadopoulos, M.; Vavourki, H.; Terzis, A.; Hountas, A.; Chiotellis, E. *Inorg. Chim. Acta* **1991**, *189*, 219−224.

Table 3. ^{1}H NMR Chemical Shifts (ppm) in D_2O for the Anionic Forms of the DD and *anti*-DL Isomers of ReO(TMEC)[a]

	pen$_b$					pen$_t$				
monanions	H_α	Me′	Me″	$H_{en'}$	$H_{en''}$	H_α	Me′	Me″	$H_{en'}$	$H_{en''}$
anti-DL	3.69	1.56	1.87	3.61	4.04	4.10	1.88	1.72	4.42	3.04
DD	3.29	1.51	2.05	3.60	2.84	4.07	1.94	1.64	4.01	3.67

	syn-pen					*anti*-pen				
dianions	H_α	Me′	Me″	$H_{en'}$	$H_{en''}$	H_α	Me′	Me″	$H_{en'}$	$H_{en''}$
anti-DL						4.13	1.77	1.48	4.17	3.48
anti-DL						3.75	1.47	1.82	3.65	3.99
time-averaged[b]						3.96	1.60	1.66	3.88	3.73
DD	2.73	1.41	1.81	4.09	2.50	4.38	1.50	1.81	3.68	3.54

	syn-pen					*anti*-pen				
trianions	H_α	Me′	Me″	$H_{en'}$	$H_{en''}$	H_α	Me′	Me″	$H_{en'}$	$H_{en''}$
anti-DL						4.04	1.53	1.70	3.89	3.48
DD	3.55	1.34	1.82	3.95	3.02	4.11	1.52	1.67	3.95	3.52

[a] Prime (′) designates atoms or groups near (endo) to the oxo atom; double prime (″) designates atoms or groups away (exo) from the oxo atom. [b] Time-averaged shifts are experimental values.

peaks from these ^{13}C signals to en protons allow us to distinguish H_{enb} from H_{ent} signals. The strongly coupled signals were assigned to the protons with the trans torsion angle ($H_{enb'}-C_6-C_7-H_{ent''}$), and the weakly coupled signals were assigned to the en protons with the gauche torsion angle ($H_{enb''}-C_6-C_7-H_{ent'}$) in the solid state. The $Me_{t'}$ and $Me_{t''}$ signals were differentiated by comparing their chemical shifts with those of the analogous signals in [ReO(DD-$TMECH_2$)]$^-$ (Table 3). As for [ReO(DD-$TMECH_2$)]$^-$, the downfield Me_t signal was assigned to $Me_{t'}$.[2]

Assignments for the dianion were determined by following the signals that shifted only slightly as monoanion converted to dianion; these are the two H_α, two H_{enb}, and two Me_b signals of the monoanion. The remaining signals for the dianion (two Me and two H_{en} signals) were assigned by analyzing the shifts of pairs of signals at pH 8.3 and those of the time-averaged signals at pH 10.8. For example, there is an H_{en} signal at pH 10.8 (3.73 ppm) that is at the midpoint of two H_{en} signals at pH 8.3 (3.48 and 3.99 ppm). The latter signal (3.99 ppm at pH 8.3) is an $H_{en''}$ signal; this signal corresponds to the $H_{enb''}$ signal in the monoanion and shifts only slightly as monoanion converts to dianion. Thus, the signals at 3.48 ppm (pH 8.3) and at 3.73 ppm (pH 10.8) are also $H_{en''}$ signals. The signals of the trianion were assigned by comparing their shifts with those of the analogous signals from the *anti*-pen residue of [ReO(DD-TMECH)]$^{3-}$ (Table 3).[2] Signals with similar shifts were given corresponding assignments.

pH Dependence. The neutral form of **1** converts to the monoanion between pH 3 and 5, coinciding with an upfield shift of the $H_{\alpha b}$ signal (not shown) and consistent with deprotonation of the uncoordinated CO_2H, since no other signals shift appreciably. ^{1}H NMR spectra at pH values ≥5.7 are shown in Figures 2 and 3. At pH 5.7 the monoanion is fully formed and the signals are sharp. At pH 6.5 and above, line broadening of all signals was observed. The roughly equal broadening of all signals at pH values up to ∼7, where the complex is far from fast exchange, suggests that one rate process is determining the rate. Between pH 7.0 and 7.9 the two H_{ent} signals collapsed into the baseline and two new broad H_{ent} signals emerged (Figure 2). The H_α and H_{enb} signals shifted only slightly (≤0.06 ppm) (Table 3). The Me signals broadened also. From pH 6.5 to 7.4 the Me signals became less symmetrical, suggestive of the decline of some original signals and the emergence of new

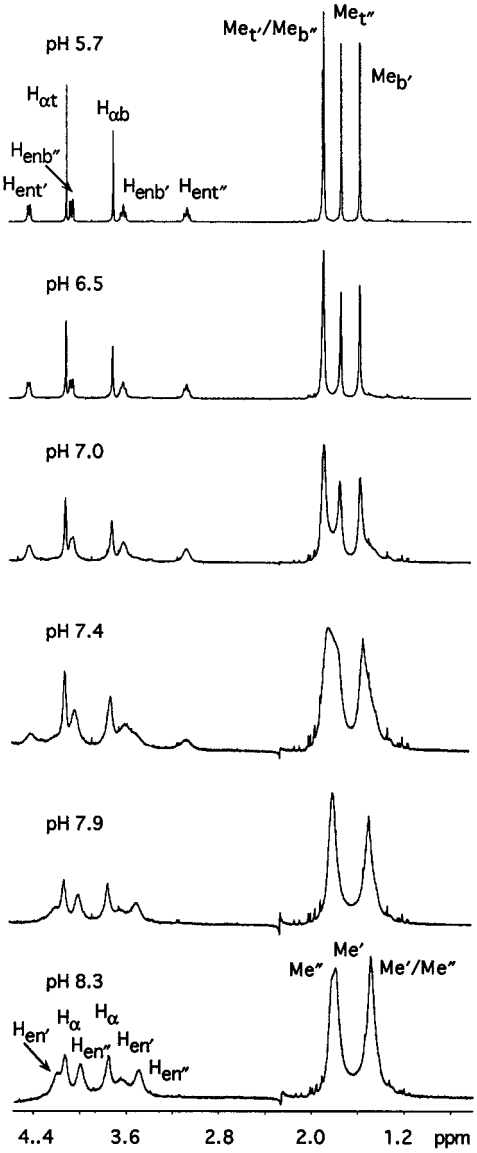

Figure 2. ^{1}H NMR spectra of *anti*-ReO(DL-$TMECH_3$) (**1**) in D_2O from pH 5.7 to 8.3.

Me signals. From pH 7.4 to 7.9, the four Me signals had coalesced to only two resolved signals of unequal intensity. As the pH was raised to 8.3, the two Me signals sharpened and equalized in intensity; then at pH 8.3, the downfield Me signal was partially resolved into two peaks. The changes in the Me region are consistent with the collapse and replacement of the original Me_t signals, while the Me_b signals shift slightly (<0.1 ppm). To summarize, the original two Me_t and two H_{ent} signals show the greatest degree of broadening and are replaced by new signals at significantly different chemical shifts. Six signals (the two H_α signals, and the original two Me_b and two H_{enb} signals) do not shift very much, and the broadening is less severe. These results are consistent with conversion of the monoanion to a dianion and an intermediate rate of monoanion/dianion exchange on the NMR time scale.

The signals of the dianion were sharpest at pH 8.3; above this pH the signals re-broadened (Figure 3). From pH 9.8 to 10.2 the Me signals merged into one broad upfield signal. Simultaneously, the H_α and H_{en} signals coalesced into a single broad downfield signal. At pH 10.8, some resolution had occurred, revealing half of the number of signals as found at pH 8.3. These new signals were at the midpoint of two signals

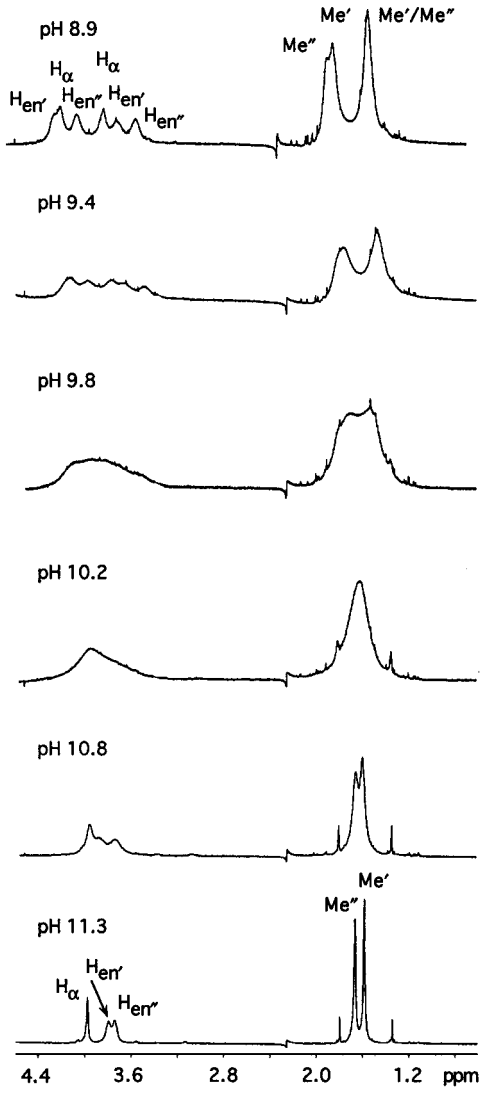

Figure 3. ^{1}H NMR spectra of *anti*-ReO(DL-TMECH$_3$) (**1**) in D_2O from pH 8.9 to 11.3.

of the same type (H_α, H_{en}, Me) at pH 8.3, indicating time-averaging between the halves of the DL-TMEC ligand but no change in protonation state. Thus, throughout this range the dianion dominates. At higher pH values (11.3 and above, not shown), the time-averaged signals continued to sharpen but also shifted, indicating conversion of the dianion into a trianion. In addition, above pH 10, there is evidence of the anti isomer converting to the syn derivative. The Me signals of the syn isomer[3] are noticeable in all spectra at pH $\geq$ 10.2 (Figure 3); one signal is upfield and one signal is downfield of the Me signals of **1**. If present below pH 10.2, these signals would overlap with the very broad signals of the anti isomer and would not be detected. Since the spectra were recorded in sequence of increasing pH, the results show that anti to syn conversion proceeds at an observable rate at least at pH values >10.

Resonance Raman Spectroscopy. The Re=O stretching frequency of **1** was monitored as a function of pH in D_2O (Figure 4). In the pH region characteristic of the monoanion as observed by NMR, a single sharp band was observed at 964 cm^{-1}. Above pH 8, in the pH region where the dianion dominated, two new mid-frequency bands (933 and 923 cm^{-1}) of approximately equal constant intensity were observed (Figure 4). From pH 11−12, these two bands declined and were replaced by a band at 891 cm^{-1} of a higher pH form (not shown). The high pH band was unsymmetrical, having a lower frequency

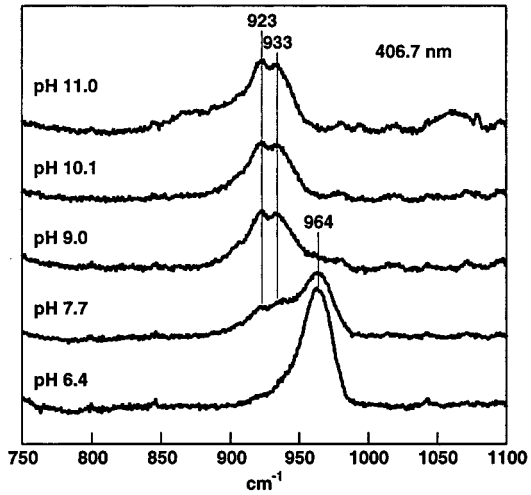

Figure 4. Resonance Raman spectra of *anti*-ReO(DL-TMECH$_3$) (**1**) in D_2O at various pH values.

Scheme 2. Equilibria of Anti Isomers of Complexes with *meso*-EC-Type Ligands

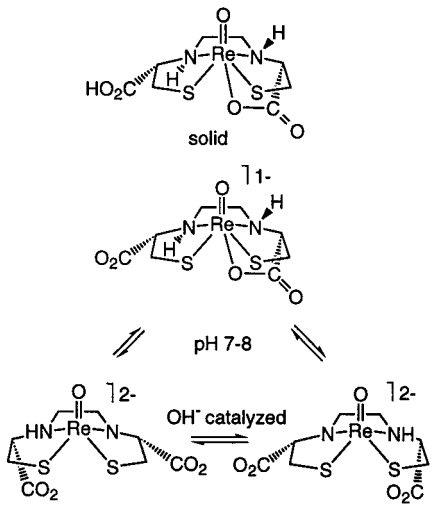

shoulder band at ~870 cm^{-1}. Over time at pH 12.5, the intensity of the high pH band decreased, and the intensity of the shoulder increased. After 8 h there were two maxima of roughly equal intensity. After 3 days only the lower frequency band (871 cm^{-1}) of *syn*-[ReO(DL-TMEC)]$^{3-}$ was observed.[3]

Incubation of **1** in $H_2{}^{18}O$ at pH 12.5 resulted in complete conversion to the *syn*-[Re^{18}O(DL-TMEC)]$^{3-}$ (830 cm^{-1}). No isotopic exchange was detected for *syn*-[ReO(DL-TMEC)]$^{3-}$ incubated in $H_2{}^{18}O$, pH 12.5, for ~6 h.

Discussion

In their neutral solid-state forms and in aqueous solution at low pH, the gross structural features of *anti*-ReO(DL-TMECH$_3$) (**1**) (Scheme 2) are more similar to those of ReO(LL-ECH$_3$) (Scheme 1) and ReO(DD-TMECH$_3$)[2] than to those of *syn*-ReO(DL-TMECH$_3$).[3] In the solid state, the latter has an unusual N_2-SO basal donor set with one CO_2^- coordinated in the equatorial plane, whereas the other complexes have the usual N_2S_2 basal donor set and a ligated CO_2 trans to the oxo ligand. In solution, deprotonation of the dangling CO_2H in all three isomers gives monoanionic complexes with the same six-coordinate geometry as found in the solid state.

Near neutral pH, the monoanion of each isomer reacts with OH^- to give dianionic forms. For ReO(LL-ECH$_3$) and ReO(DD-

$TMECH_3$), we observed severe NMR signal broadening in the pH range 6−8.[2,12] We believe that OH^- deprotonates the NH of the cys_t/pen_t residue in the monoanion, resulting in an *anti*-CO_2^- deligated dianion (Scheme 1).[2] Because NH dissociation (which is normally fast) is coupled to the slower CO_2^- deligation step, the rate of equilibration between the mono- and dianionic forms is comparable to the NMR time scale, explaining the broadening. However, since OH^- can act as a ligand, OH^- may bind to Re, replacing the axially bound CO_2^-, rather than deprotonate the complex. The low symmetry of the M(V)═O(N_2S_2) complexes with chiral N_2S_2 ligands does not allow an unambiguous distinction between these two roles for OH^-.

For *syn*-ReO(DL-$TMECH_3$), the monoanion to dianion reaction is slow since both a chelate ligand rearrangement and CO_2^- deligation must occur. The reacting monoanion has an N_2SO basal coordination, and the NMR spectral properties of the monoanion, combined with Raman data, allowed us to establish that the role of OH^- was NH deprotonation, not axial ligation. As shown in Chart 2, the disposition of both carboxyl groups to one side of the coordination plane bestows some similar characteristics to the syn and anti isomers of ReO(DL-$TMECH_3$). In fact, although the chelate ligand is a meso isomer, each ligand can coordinate in such a way as to form chiral complexes. In the syn isomer, the chirality uniquely arises from the ligand forming a dianionic complex with one nitrogen retaining the proton (NH) and one nitrogen losing its proton (forming a coordinated nitrogen having a lone pair (NLp). These differences in the ligand nitrogen donors break the mirror plane, giving a racemic mixture of enantiomers; each enantiomer has the same NMR signals (just two sets of pen signals). Since the dianion of the syn isomer cannot have an axially ligated CO_2^- group, the anti isomer studied here is a better model for the isomers with the chiral (DD and LL) ligands (cf., Schemes 1 and 2). Coordination of only one of the two carboxyl groups breaks the mirror plane, and thus the anti isomer is formed as a mixture of the two enantiomers. [At this point of the discussion, we present only a simplified view of the solid and aqueous solution states of anti meso EC-type ligands. Only the enantiomer of *anti*-ReO(DL-ECH_3) with the carboxyl of the L residue coordinated is shown in Scheme 2. Of course, the other enantiomer is equally abundant. If these equilibria are fast, one expects to observe just one set of pen NMR signals since the coordinated carboxyl group within each complex would alternate rapidly between the D and the L residue.]

A ligated NH group can have one of two configurations, with the hydrogen endo or exo to the oxo group. At low pH, there is only one set of signals for each pen residue of *anti*-ReO(DL-$TMECH_3$), indicating that the two ligated NH groups each favor one configuration at N. The shift of the NMR signal of one H_α is clearly indicative of a "tridentate" pen residue with the carboxyl coordinated to an axial position. The shift of the NMR signal of the other H_α was consistent with deprotonation of a dangling carboxyl group. Raman data for *anti*-ReO(DL-$TMECH_3$) (**1**) were simple and definitive. The Re═O band of the monoanion (964 cm^{-1}) was replaced from pH 7−8 by two Re═O bands for the dianion (933 and 923 cm^{-1}) (Figure 4). No further changes were observed until above pH 11. Therefore, the NMR spectral changes observed for **1** from pH 6.5−8.3 (Figure 2) arise from the monoanion to dianion conversion. Changes included line broadening and the replacement of some original signals with new ones. For those signals for which the shift differences are large between mono- and dianion, the line broadening is severe. Thus, monoanion/dianion equilibration proceeds at a moderate rate on the NMR time scale. Since this behavior is similar to that observed for ReO(DD-$TMECH_3$) near pH 7.0 and is consistent with CO_2^- deligation/ligation, we conclude that reaction of the monoanion of **1** with hydroxide leads to CO_2^- deligation.

Scheme 3. NH-Deprotonated Dianions of Anti Isomers of Complexes with *meso*-EC-Type Ligands

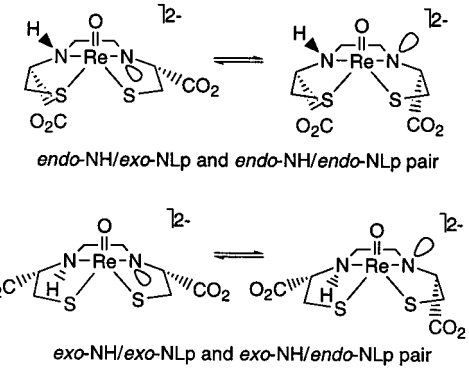

The frequencies of the Raman Re═O bands for the dianion of *anti*-ReO(DL-$TMECH_3$) (**1**) are consistent with either NH deprotonation or OH^- ligation.[2,5,6] Since there are two bands of constant intensity, the correct formulation for the dianion must account for a constant mixture of two forms. The intensities of the bands suggest nearly equal amounts of the two forms. However, Raman band intensity depends on many factors, and the two forms could have different abundances. Possibilities for the dianion include (i) two NH-deprotonated isomers or conformers, (ii) two hydroxo-ligated isomers, or (iii) a mixture of one NH-deprotonated and one hydroxo-ligated form.

Can we distinguish between these possibilities on the basis of the results obtained for **1**? We consider first the most reasonable possibility, (i) two NH-deprotonated dianions. The NH-deprotonated dianion has one N^- donor that carries a lone electron pair (NLp), and one neutral N donor that carries a proton (NH). Both the NH and NLp can be either endo or exo to the oxo ligand. Thus, four NH-deprotonated forms are hypothetically possible: *endo*-NH/*endo*-NLp, *endo*-NH/*exo*-NLp, *exo*-NH/*endo*-NLp, and *exo*-NH/*exo*-NLp. Each form is dissymmetric, i.e., the halves of the TMEC ligand are not equivalent, and thus each half could have its own set of NMR signals. (Each form exists as an enantiomeric pair; the consequences of enantiomers are discussed below.) The four possible NH-deprotonated forms can be grouped into two pairs of conformers (Scheme 3); the members of each pair have the same NH orientation and differ only in the orientation of the NLp. Thus, the partners can interconvert simply by NLp inversion. Since NLp inversion is ordinarily very fast (faster than the time scale of an NMR experiment), the partners will have time-averaged NMR signals. However, the two partners will give two Raman bands since the time scale for resonance Raman spectroscopy is much faster than that for NMR spectroscopy. Since many steps are involved in an interpair conversion, no member of one pair will interconvert rapidly with a member of the other pair (in the absence of a catalyst, see below). Thus, if both pairs are present, we should see four sets of pen signals. Since only two sets of pen signals were observed, we conclude that only one of these two pairs exists in solution.

Since there is evidence for only one pair of conformers for the dianion, we must choose between the pairs. We exclude the *exo*-NH/*exo*-NLp and *exo*-NH/*endo*-NLp pair (bottom, Scheme 3) because empirical evidence indicates that in [M(V)═O]$^{3+}$ complexes an *endo*-NH is preferred,[10] probably for steric reasons. In addition, a complex with an *exo*-NH/*exo*-NLp

Scheme 4. Exchange of NH and NLp Sites in the Anti Isomers of Complexes with *meso*-EC-Type Ligands

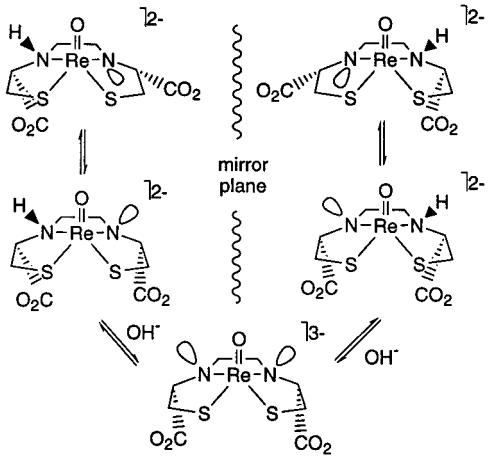

Chart 5. Hydroxo-Ligated Dianions of Anti Isomers of Complexes with *meso*-EC-Type Ligands

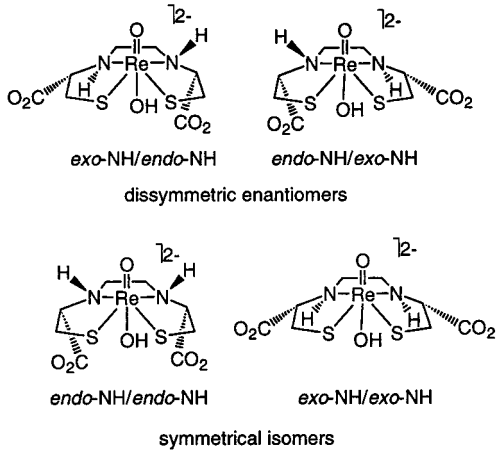

configuration is likely to be severely conformationally strained. The two chelate ring C's bound to each ligated N will be positioned above the basal plane, and the TMEC ligand will form a pocket around the coordinated metal. The $[M(V)=O]^{3+}$ group is normally apical, and thus the *exo*-NH/*exo*-NLp conformer is unlikely to exist in a significant concentration. Thus we conclude that the dianion consists of the *endo*-NH/*exo*-NLp and *endo*-NH/*endo*-NLp pair (top, Scheme 3). In previous work, we found that *syn*-[ReO(DL-TMECH)]$^{2-}$ also exists as a pair of *endo*-NH/*exo*-NLp and *endo*-NH/*endo*-NLp conformers and that NLp inversion equilibrating these forms is fast on the NMR time scale.[3]

In summary, the data indicate that the dianion of **1** is a mixture of two NH-deprotonated conformers. We discussed the presence and interconversion of the two conformers of the dianions of **1**. However, each conformer exists as an enantiomeric pair since either the D-pen or the L-pen residue can be protonated at N. The presence of enantiomers leads to a simple explanation for the fluxional behavior of the dianion observed by NMR spectroscopy. The NH and N^- sites exchange through a base-catalyzed mechanism. Such a process is shown stepwise in Scheme 4. Beginning with the *endo*-NH/*exo*-NLp conformer (top left-hand corner in Scheme 4), inversion of the NLp (which is fast and pH independent) gives the conformer with the same stereochemistry at both N's, *endo*-NH/*endo*-NLp (middle-left, Scheme 4). In the next step (shown at the bottom of Scheme 4), OH^- deprotonates the original NH site to give an undetectable amount of a symmetrical trianionic intermediate. This intermediate is rapidly protonated to re-form the dianion. If the N on the right side of the trianionic intermediate is protonated, the corresponding enantiomers, *endo*-NLp/*endo*-NH and *exo*-NLp/*endo*-NH (shown at the right of Scheme 4), are formed. This overall process is slow to intermediate on the NMR time scale when the concentration of the catalyst, OH^-, is low (pH < 10). However, when the concentration of OH^- is high (pH > 10), the process becomes fast and the signals from the inequivalent halves of the complex become time averaged. Similar behavior was observed for the dianion of *syn*-ReO(DL-$TMECH_3$).[3]

The other possibilities, (ii) two hydroxo-ligated forms only and (iii) a mixture of NH-deprotonated and hydroxo-ligated forms, can be assessed with the spectral data. For ii and iii to be consistent with two equally intense sets of pen NMR signals and two Raman bands, a mixture of two forms must be present. The mixture could have equally stable symmetrical forms in slow exchange or a dissymmetric form in fast exchange with the second form. We explain below.

The hypothetical isomers that are possible for a hydroxo-ligated dianion are depicted in Chart 5. Again, these arise because the NH's can be either endo or exo to the oxo ligand. The dissymmetric form would satisfy the NMR criteria but not the Raman criteria. Two hypothetical hydroxo-ligated forms would be symmetrical isomers (*endo*-NH/*endo*-NH and *exo*-NH/*exo*-NH). Each will have one unique set of pen NMR signals and one unique Re=O Raman band. Both would have to be present to satisfy the NMR requirement of two equally abundant symmetrical forms in slow exchange. However, if the monoanion converted to two dianions having separate signals as required by this version of possibility ii, each monoanion H_α must exchange with the H_α's in both dianions. Both monoanion H_α signals must become relatively broad since each monoanion H_α signal has a shift significantly different from one of the dianion H_α signals. However, the H_α signals remain relatively sharp (Figure 2). Thus, we exclude this version of possibility ii. A mixture of the dissymmetric- and one symmetrical-hydroxo form can be excluded for the same reason.

Next we consider possibility iii, a mixture of one NH-deprotonated and one hydroxo-ligated form. All four possible NH-deprotonated dianions are dissymmetric (Scheme 3) and will have two sets of pen NMR signals in the absence of averaging. Therefore, any of the four could be in fast exchange with the dissymmetric hydroxo-ligated dianion. Only the appropriate enantiomers of the NH-deprotonated and hydroxo-ligated forms would interconvert rapidly since some enantiomeric interconversion would average the signals from the halves of the DL-TMEC ligand. Thus, the spectral data can be explained since there could be two Raman bands and the two equally intense sets of pen signals.

Possibility iii could be ruled out in the case of the syn isomer, *syn*-[ReO(DL-TMECH)]$^{2-}$, due to its more rapid rate of NH exchange under acidic conditions and the slow rate of the complicated CO_2^- deligation process.[3] For the anti isomer studied here, we cannot strictly rule out this possibility. However, possibility iii is unlikely for several reasons. First, it does not occur for the syn analogue. The syn isomer's NLp has both endo and exo orientations in different conformers, whereas possibility iii almost demands a stereospecific orientation with one NLp orientation leading to one favored conformer. Second, the two conformers of the dianionic syn species have Re=O bands at 942 and 929 cm^{-1}, similar to the 923 and 933 cm^{-1} values found here for the anti isomer. Finally, we have

Scheme 5. Anti to Syn Conversion of a Hydroxo-Ligated Dianion of Complexes with *meso*-EC-Type Ligands

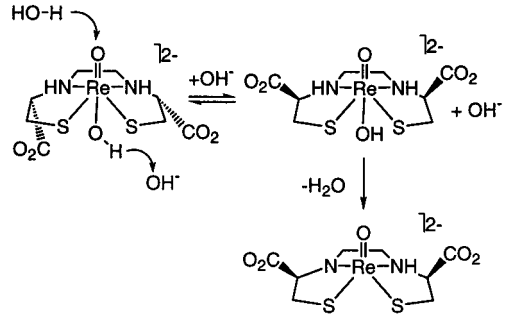

shown that interconversion of oxo and hydroxo ligands in $[ReO(OH)(penH_2)_2]^{2-}$ and $[ReO(OH)(dioxo\text{-}tetH_4)]$ is extremely facile.[5,6,18] For $[ReO(OH)(penH_2)_2]^{2-}$, ^{18}O exchange was too fast above pH 7 to measure by resonance Raman spectroscopy, even though the concentration of the hydroxo-ligated form of the complex does not reach 50% until the pH is raised to 11.8. For both $[ReO(OH)(penH_2)_2]^{2-}$ and $ReO(OH)(dioxo\text{-}tetH_4)$ (pH > 6), exchange of the oxo and hydroxo ligand sites was fast on the NMR time scale, giving time-averaged signals for the geminal pairs of methyl groups and protons in the pen and dioxo-tet ligands, respectively. Although the symmetry does not allow us to detect such time averaging of signals of geminal proton pairs, we would detect an anti to syn isomerization. None was observed below pH 10.

Above pH 10, **1** slowly converts to the syn isomer. Since the pK_a of the dianion of **1** is ~11, the dianion of **1** is present under conditions in which isomerization occurs. If the dianion were the hydroxo-ligated form (Scheme 5), it should isomerize extremely rapidly. In the first step, oxo/hydroxo exchange essentially converts the anti isomer to a hydroxo-ligated form of the syn isomer. In the second step, loss of H_2O (OH^- deligation and NH deprotonation) gives the stable form of the syn isomer.[3] Oxo/hydroxo exchange should be very fast. Since there was no evidence of ^{18}O exchange in *syn*-ReO(DL-$TMECH_3$) for up to 6 h, a hydroxo-ligated form of the syn isomer must be highly disfavored and must have a high rate of OH^- deligation. Thus, if the dianion were mainly a hydroxo-ligated species, neither step is likely to be slow enough to reasonably account for the observed slow rate of isomerization. The hydroxo-ligated form is not the stable form of the dianion.

The hydroxo-ligated form leading to isomerization is either an intermediate or an activated complex on the reaction pathway for isomerization. The hydroxo species is formed in a slow step from the trianion of **1**, which is most likely a five-coordinate species with both N's deprotonated (Scheme 6). At pH 7, the preparative reaction using the DL+DD+LL-ECH_6 isomeric mixture results in ~30% of the $ReO(ECH_3)$ complex being the *anti*-ReO(DL-ECH_3) product. When the pH of the reaction solution is raised to 12, conversion of *anti*-ReO(DL-ECH_3) to the syn isomer is complete in less than 20 min. Conversion of **1** is much slower, probably because the Me″ groups of the TMEC ligand hinder attack by incoming hydroxide. We propose that, once hydroxide adds to the complex, oxo/hydroxo ligand exchange and loss of OH^- proceed rapidly to give the stable syn isomer.

Isolation of a single isomer by kinetic control in a preparative reaction is usually not possible. Thus, the essentially complete anti to syn conversion of EC-type complexes at equilibrium is

Scheme 6. Anti to Syn Isomerization of the NH-Deprotonated Trianion of Complexes with *meso*-EC-Type Ligands

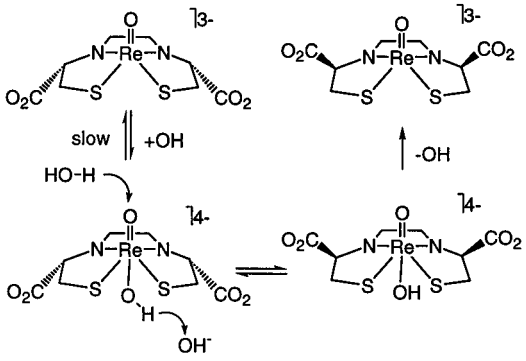

advantageous since a single isomer can be obtained directly from the reaction solution. Preference for the syn isomer is significant because syn isomers of ^{99m}Tc-based renal agents usually have a higher rate of renal clearance compared to their anti counterparts.[19] Thus, understanding the factors that allow anti to syn equilibration and control the equilibrium position of the EC-type complex should be extremely helpful in the design of useful new agents. The rate of equilibration is also important since clinical preparation of radiopharmaceuticals should not exceed ~30 min.

Previously, studies of anti isomers with carboxyl groups were limited to those in which the isomers do not equilibrate.[8,19] Thus, their relative thermodynamic stability could not be determined. In the exceptional case of $ReO(D\text{-}penH_2)(L\text{-}penH_3)$, only the anti isomer is known.[6] For pairs of syn and anti isomers that do equilibrate, only the syn isomers have been studied in detail because the anti isomers are relatively unstable and difficult to isolate.[3,7] However, the combined information from these studies led to important conclusions. We now state each of these previous conclusions and assess how well they are supported by our new results.[7]

First, pairs of syn and anti isomers equilibrate only if the complexes are flexible, and amine donors impart flexibility. *anti*-ReO(DL-$TMECH_3$) (**1**) converts to the syn isomer. In the X-ray crystal structure of **1** (Figure 1) all three chelate rings are anchored by an amine and are highly puckered, indicating a high degree of flexibility. Second, ligated amines prefer the endo configuration and thus the amine must be able to invert for equilibration to occur. Under conditions in which isomerization of **1** occurs, the trianion of **1** is present. This result does not eliminate the possibility that the dianion of **1** converts to the syn isomer, and that the observable rate of isomerization above pH 10 depends on hydroxide concentration alone. However, this result is more consistent with the conclusion that isomerization requires inversion of amine donor chirality; such inversion is preceded by amine donor deprotonation.

Finally, we have concluded that syn isomers are thermodynamically preferred over anti isomers because an anti carboxyl group (attached to a carbon bound to an anchoring amine with an endo configuration) is drawn in toward the metal coordination sphere. The short-range interaction between an (uncoordinated) anti carboxyl group and the metal coordination sphere is highly unfavorable. Thus, the amine donors in the anti isomers adopt an exo configuration. The destabilizing effect of the exo amine configuration in the anti isomer favors the syn isomer. In the

(18) Hansen, L.; Lampeka, Y. D.; Gavrish, S.; Xu, X.; Taylor, A. T.; Marzilli, L. G. *Inorg. Chem.*, in press.

(19) Rao, T. N.; Adhikesavalu, D.; Camerman, A.; Fritzberg, A. R. *J. Am. Chem. Soc.* **1990**, *112*, 5798−5804.

solid state, **1** (Figure 1) has an *exo*-NH. The exo configuration of N(1) extends the uncoordinated carboxyl group away from the metal coordination sphere. The destabilizing effect of the *exo*-NH makes the anti isomer unstable with respect to the syn isomer.

We can expand the third conclusion to explain why the equilibrium positions of the EC- and MAEC-type complexes differ. For the EC-type complex, the anti isomer does not exist in a detectable concentration at equilibrium. The anti isomer of ReO(MAECH$_2$) accounts for 6% of the complex at equilibrium.[7] *anti*-ReO(MAECH$_2$) has only one carboxyl group. The EC-type complexes have two carboxyl groups. The coordinated carboxyl group in the solid and the monoanion of **1** is probably not destabilizing since deligation occurs at a relatively high pH ($\sim$7.5), and the only known isomer of ReO(D-penH$_2$)(L-penH$_3$) has a coordinated carboxyl group. However, in the dianion and trianion of **1**, both anti carboxyl groups are uncoordinated. The *exo*-NH/*exo*-NLp dianion and the *exo*-NLp/*exo*-NLp trianion are likely to be severely conformationally strained and probably do not exist. For all other possible conformers, at least one carboxyl group will be drawn in toward the metal coordination sphere. The destabilization from the interaction between the carboxyl group and the metal coordination sphere (with or without an exo configuration at one amine) in the *anti*-EC-type complexes is probably greater than the destabilization of only an exo amine configuration in *anti*-ReO(MAECH$_2$).

Conclusion

The dianion of *anti*-ReO(DL-TMECH$_3$) (**1**) is most likely a mixture of two NH-deprotonated conformers, as was found for the syn isomer.[3] In addition, the similar Re=O band frequencies and pK_a values for the dianions of **1** ($\nu_{Re=O}$ = 933, 923 cm^{-1}; pK_a $\approx$ 11) and ReO(DD-TMECH$_3$) ($\nu_{Re=O}$ = 930 cm^{-1}; pK_a $\approx$ 11) provide evidence that the dianions of the latter type (i.e., having the chiral ligands) are also NH-deprotonated forms. The destabilizing effect of short-range interactions between the uncoordinated carboxyl groups and the metal coordination sphere (with or without an exo configuration at one amine) makes the anti isomer of ReO(DL-TMECH$_3$) unstable with respect to the syn isomer.

Acknowledgment. This work was supported by the National Institutes of Health (grant no. DK38842). We thank Professor Teizo Kitagawa (Institute for Molecular Science, Japan) for the use of resonance Raman instrumentation, Dr. Kwok To Yue for collecting the ^{18}O resonance Raman spectra, and Dr. Patricia A. Marzilli for her invaluable comments.

Supporting Information Available: Crystallographic data for **1** (crystal data and experimental parameters, atomic coordinates with equivalent isotropic displacement coefficients, complete tables of bond lengths and bond angles, anisotropic displacement coefficients, and H-atom parameters). Crystallographic data, in CIF format. This material is available free of charge via the Internet at http://pubs.acs.org.

IC000183Q